Pergamon

Tetrahedron Letters 39 (1998) 2985–2988

TETRAHEDRON LETTERS

# Chiral Recognition of 1,1'-Bi-2-naphthol Enantiomers by Twisted Amidine Derivatives: Rational Design of a Highly Enantioselective Receptor

**Yasuo Dobashi*, Kiyotaka Kobayashi, Norihisa Sato, and Akira Dobashi***

Tokyo University of Pharmacy & Life Science, School of Pharmacy,
1432-1 Horinouchi, Hachioji, Tokyo 192-0392, Japan

Received 19 January 1998; revised 7 February 1998; accepted 10 February 1998

***Abstract***: Clarification of the molecular structures of diastereomeric complexes relevant to the enantioselective dual N···HO bonding between the chiral $C_2$ amidine derivative (*S,S*)-**1** and 1,1'-bi-2-naphthol **2** in $CDCl_3$ afforded the structural factor determining the sense of observed enantioselection. This insight into chiral recognition was successfully applied to the design of a new twisted dual hydrogen bond acceptor (*S,S*)-**3** that exhibited a higher level of enantioselectivity toward **2**.


The molecular structures of the transient diastereomers underlying the enantioselective complexation are of fundamental importance in gaining insight into chiral molecular recognition.[1] We recently developed the amidine-based $C_2$ receptor (*S,S*)-**1** capable of recognizing the molecular chirality of a series of aliphatic diols through dual $N^{im}$···HO interactions in $CDCl_3$.[2] The major feature of (*S,S*)-**1** as a dual acceptor for hydrogen bonding is its binding surface where a pair of imino nitrogens create the twisted intermolecular dual hydrogen bonding. The basis of enantioselectivity generated by (*S,S*)-**1** lies in the formation of diastereomers, the component molecules of which are held together with a different twist in their orientation.[3] In the present study, the enantioselective complexation of (*S,S*)-**1** with 1,1'-bi-2-naphthol **2** and the binding geometry of hydrogen-bonded complexes relevant to the enantioselectivity are explored. On the basis of the structural factor responsible for the sense of enantioselectivity, the highly selective receptor (*S,S*)-**3** for a enantiomeric pair of **2** is developed.

Table 1 summarizes thermodynamic parameters for complexation between (*S,S*)-**1** and each single enantiomer of **2** in $CDCl_3$. The stoichiometry of each diastereomeric complexation was determined to be 1:1 by Job's plot based on the change in the absorbance of the free OH stretching band. Association constants were assessed through the non-linear least squares regression of a set of shift data obtained by $^1H$ NMR titration. In the experiments, the concentration of a single enantiomer of **2** was kept constant and that of (*S,S*)-**1** was gradually increased with monitoring the shift change of $H_4$ of **2**. The modest but definitive (*S*)-selectivity of (*S,S*)-**1** toward **2** was confirmed with $\Delta(\Delta G)$ = 340 cal/mol at 298 K and 540 cal/mol at 263 K. A van't Hoff plot using association constants obtained at four different temperatures revealed large enthalpy changes exceeding 10 kcal/mol in both diastereomeric complexations, suggesting the dual N···HO bonding. This binding mode for the two systems was well supported by the intermolecular NOE correlation observed between the methine protons of (*S,S*)-**1** and hydroxyl protons of a single enantiomer of **2** in an equimolar solution (each 8 mM) of these species in $CDCl_3$ at 283 K, as indicated in the table figure. Under these conditions, the hydroxyl protons ($\delta_{free}$ 5.04) of **2** appeared at 10.16 and 11.38 ppm, and complexations achieved were 79 and 85 % in the (*S,S*)-**1**-(*R*)-**2** and (*S,S*)-**1**-(*S*)-**2** system, respectively. The diastereotopic

0040-4039/98/$19.00 
*PII:* S0040-4039(98)00436-5

but isochronous methyl protons (δ 1.17) of (*S,S*)-**1** split into a pair of singlets upon complexation with **2**. The signal splitting resulted from a selective upfield shift ($\delta_1$ 1.03, $\delta_2$ 1.21) in the (*S,S*)-**1**-(*R*)-**2** system. In contrast, a selective downfield shift ($\delta_1$ 1.18, $\delta_2$ 1.44) was noted for the resonance of the methyl protons in the more stable (*S,S*)-**1**-(*S*)-**2** system. In addition, intermolecular NOE was definitively detected between $H_3$ of (*S*)-**2** and the downfield methyl singlet of (*S,S*)-**1**.

Table 1 Thermodynamic parameters for enantioselective complexation of (*S,S*)-**1** with enantiomers of 1,1'-bi-2-naphthol **2**, intermolecular NOE correlations and shift changes observed in $CDCl_3$.[a,b]

| | (*R*)-**2** | (*S*)-**2** |
|---|---|---|
| *K* at 298 K ($M^{-1}$) | 785 | 1400 |
| *K* at 263 K ($M^{-1}$) | 8200 | 23200 |
| $\Delta H$ (kcal/mol) | -10.5 | -12.6 |
| $\Delta S$ (e.u.) | -21.9 | -27.9 |

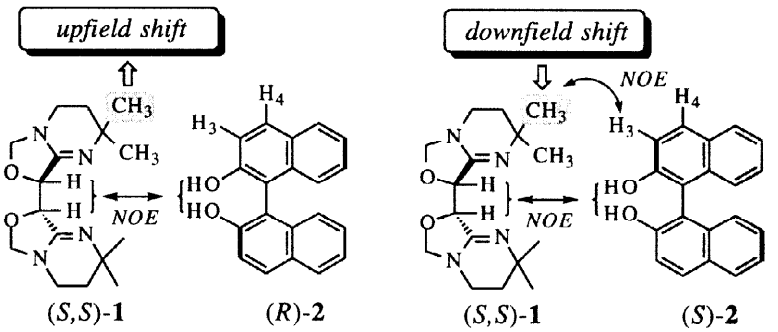


a) Errors in association constants at 298 K were below 5%. Errors in those at 263 K were increased to 16 and 38 % for (*R*)- and (*S*)-**2**. b) NOE correlations and shift changes for the symmetry related protons are omitted for clarity. NOEs above 10% enhancement of signal intensity are cited.

For the (*S,S*)-**1** and (*S*)-**2** system, the molecular structure that embodied the above spectral features was demonstrated by X-ray analysis of the single crystal of a 1:1 complex comprised of these species.[4] As shown in Figure 1, the $C_2$ structure of the complex determined by the analysis of X-ray crystallographic data unambiguously shows dual N···HO interactions (N-HO = 1.670 Å, N-O = 2.627 Å) between the component molecules. In the complex, a methyl substituent of (*S,S*)-**1** is not only in close proximity to $H_3$ of (*S*)-**2**, but placed within the deshielding zone of a naphthyl ring as well. These structural features are quite consistent with NOEs and induced shift changes observed in solution. We thus conclude that this X-ray structure accounting for NMR data is equivalent to the preponderant structure of the complex in solution.

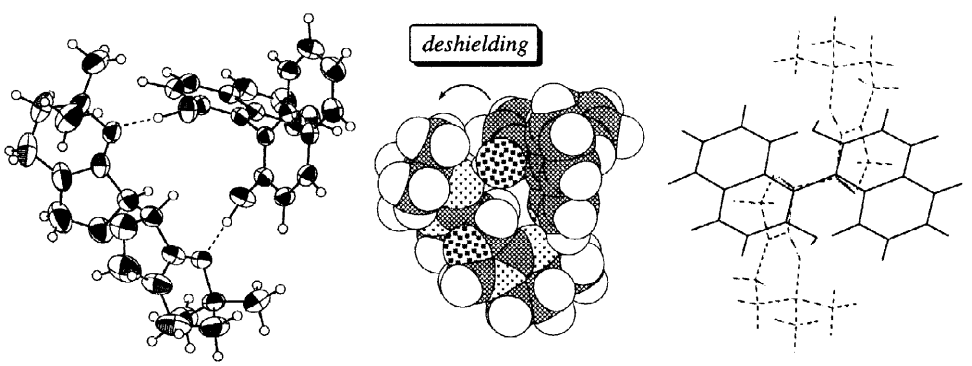


Figure 1. X-ray crystal structure of the $C_2$ complex of (*S,S*)-**1** with (*S*)-**2**. Left: ORTEP drawing of the complex. The thermal ellipsoids show 50% probability surfaces. Center: Space-filling representation of the complex reproduced by Chem 3D plus, based on the X-ray coordinates. Right: Projection of the X-ray crystal structure of the complex viewed along the $C_2$ axis from (*S*)-**2** side.

The complex of (*S,S*)-**1** with (*R*)-**2** has not been crystallized yet, but computational simulation based on the following considerations provided a candidate for the structure of the (*S,S*)-**1**-(*R*)-**2** complex formed in solution. The significant upfield shift which occurred for methyl protons of (*S,S*)-**1** upon complexation with (*R*)-**2** was most likely due to a shielding effect of the naphthyl rings of (*R*)-**2**. The binding geometry permitting such anisotropic effect apparently evolves from a structural factor, namely, that the methyl substituents of (*S,S*)-**1** are eclipsed by the naphthyl rings of (*R*)-**2**. The conformer of the hydrogen-bonded

complex featuring this structural factor was fabricated and subjected to a molecular dynamics run followed by the geometry optimization at the 3-21G(*) level, yielding the molecular structure depicted in Figure 2.[5,6] As shown in the projection of the complex, dual hydrogen bonding between (*S,S*)-**1** and (*R*)-**2** resulted in a different twist between these molecules compared with the X-ray crystal structure of its diastereomeric counterpart. Twisting in this instance established the conformation of the complex where a methyl group of (*S,S*)-**1** was arranged in the shielding region of a naphthyl ring of (*R*)-**2**, thus being consistent with solution NMR data.

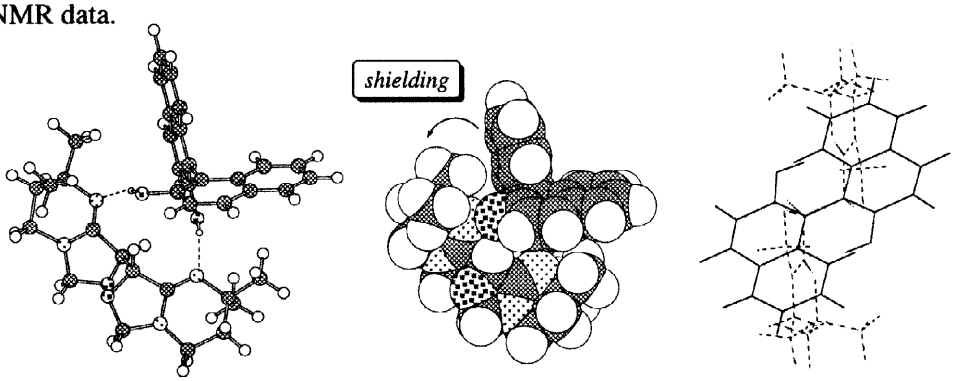


Figure 2. Calculated structure of the complex of (*S,S*)-**1** with (*R*)-**2**. All structures were regenerated by Chem 3D plus, based on the optimized coordinates at the HF/3-21G(*) level. Hydrogen bond distances (N-HO) are 1.798 and 1.802 Å. Right: Projection of the complex viewed along the pseudo $C_2$ axis from (*R*)-**2** side.

For the enantioselectivity observed in the present system, the difference in binding enthalpy by as much as 2.1 kcal/mol predominated over the entropy term, thus determining the sense of chiral recognition. Intuitively, a face approach of the naphthyl rings of (*R*)-**2** to the molecular surface of (*S,S*)-**1**, proposed as the binding motif for less stable complexation, is expected to generate higher steric interaction between the methyl groups and surfaces of the naphthyl rings. Such untoward interaction should be one factor leading to the lower binding enthalpy in the (*S,S*)-**1**-(*R*)-**2** complexation. This insight into chiral recognition dictated the construction of more effective steric barriers against the face approach of (*R*)-**2**, as a design basis of the new molecule that would exert the higher *S* selectivity toward this substrate. Accordingly, an amidine-based twisted receptor (*S,S*)-**3** was designed and synthesized.[7] In this molecule, the benzene rings are incorporated into the fused ring systems involving the amidine units. These benzene rings are expected to permit the approach of (*S*)-**2** to (*S,S*)-**3** leading to the same binding motif as observed for the more stable (*S,S*)-**1**-(*S*)-**2** system, whereas the edges of these rings in the binding sites of (*S,S*)-**3** will function as the effective steric barrier against the access of the naphthyl surface upon complexation with (*R*)-**2**. It follows, as a consequence, that (*S,S*)-**3** exhibits the higher enantioselectivity toward **2** with a larger difference in the binding enthalpy.

Table 2 Thermodynamic parameters for enantioselective complexation of (*S,S*)-**3** with enantiomers of 1,1'-bi-2-naphthol **2** and X-ray structure of a 1:1 complex of (*S,S*)-**3** with (*S*)-**2**.[a,b]

| | (*R*)-**2** | (*S*)-**2** |
|---|---|---|
| $K$ at 298 K ($M^{-1}$) | 43 | 340 |
| $K$ at 263 K ($M^{-1}$) | 290 | 6780 |
| $\Delta H$ (kcal/mol) | -8.5 | -13.2 |
| $\Delta S$ (e.u.) | -21.1 | -32.9 |

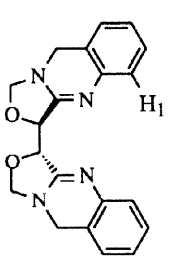


(*S,S*)-**3**

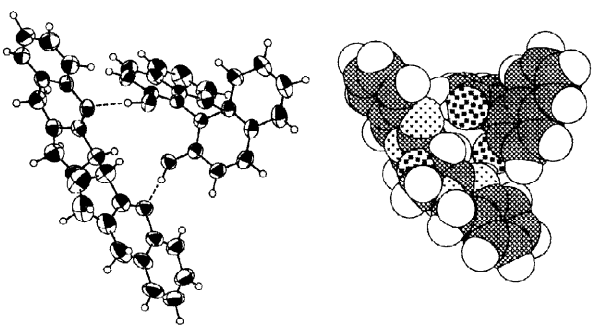

a) Error in an association constant with (*S*)-**2** at 263 K was ca. 13 %. Errors in other measurements were below 6%. b) Thermal ellipsoids were drawn at a 50% probability level. Space filling model was drawn by Chem 3D plus. Interatomic distances relevant to intermolecular hydrogen bonds are 1.865 (N-HO), 2.779 (N-O), 1.815 (N'-HO'), and 2.673 (N'-O') Å.

The thermodynamic parameters compiled in Table 2 are those measured for the complexation of (*S,S*)-**3** with the enantiomers of **2** in $CDCl_3$ by the same methods as used in the (*S,S*)-**1**-**2** system. The complexation caused the large downfield shift for the resonance of hydroxyl protons of **2**, reflecting the N···HO interaction. The limiting shift differences ($\Delta\delta$) of these nuclei at 273 K were evaluated to be 5.3 and 7.0 for (*R*)- and (*S*)-**2**. As expected, a high level of *S*-selectivity was achieved with $\Delta(\Delta G)$ = 1.2 kcal/mol at 298 K and 1.6 kcal/mol at 263 K. The difference in enthalpy change increased to 4.7 kcal/mol, supporting the validity of our design basis of (*S,S*)-**3**. In addition, the binding motif observed for (*S,S*)-**1** and (*S*)-**2** was regenerated in this new system as demonstrated by the X-ray crystal structure of (*S,S*)-**3**-(*S*)-**2** complex presented in the table figure.[8,9] The downfield ($\Delta\delta$ 0.24) and upfield shifts ($\Delta\delta$ 0.21), as the limiting values from the free species, were noted for $H_1$ of (*S,S*)-**3** and $H_3$ of (*S*)-**2** in solution (at 273 K), respectively. The molecular structure of the complex in the crystalline state makes possible the induction of such shifts by the ring currents of the aromatics.

**Acknowledgments.** We thank Mrs. T. Sakuma of this university for NMR measurements and Mr. H. Fukaya of this university for X-ray crystallographic data collection. This research was supported by a grant from the Ministry of Education of Japan (Grant-in-Aid No. 09877419).

## REFERENCES AND NOTES

1. For example, see: (a) Pirkle, W. H.; Pochapsky, T. C. *J. Am. Chem. Soc.* **1987**, *109*, 5975-5982. (b) Dobashi, Y.; Hara, S.; Iitaka, Y. *J. Org. Chem.* **1988**, *53*, 3894-3896. (c) Cristofaro, M. F.; Chamberlin, A. R. *J. Am. Chem. Soc.* **1994**, *116*, 5089-5098. (d) Dobashi, Y.; Dobashi, A.; Iitaka, Y. *Tetrahedron Lett.* **1994**, *35*, 9413-9416 and references cited therein. (e) Pirkle, W. H.; Murray, P. G.; Rausch, D. J.; McKenna, S. T. *J. Org. Chem.* **1996**, *61*, 4769-4774. (f) Pirkle, W. H.; Murray, P. G.; Wilson, S. R. *ibid.* **1996**, *61*, 4775-4777. (g) Yashima, E.; Yamamoto, C.; Okamoto, Y. *J. Am. Chem. Soc.* **1996**, *118*, 4036-4048 and excellent literature citations made therein. (h) Dearden, D. V.; Dejsupa, C; Liang, Y.; Bradshaw, J. S.; Izatt, R, M. *J. Am. Chem. Soc.* **1997**, *119*, 353-359.

2. Dobashi, Y.; Kobayashi, K.; Dobashi, A. *Tetrahedron Lett.* **1998**, *39*, 93-96.

3. Dobashi, Y.; Dobashi, A.; Ochiai, H.; Hara, S. *J. Am. Chem. Soc.* **1990**, *112*, 6121-6123.

4. Crystal data for (*S,S*)-**1**:(*S*)-**2** complex ($C_{16}H_{26}O_2N_4 \cdot C_{20}H_{14}O_2$, *Mr* 592.7): crystal system orthorhombic; space group $P2_12_12$; lattice constants, $a$ = 12.904 (5), $b$ = 11.293 (6), $c$ = 11.244 (4) Å, $V$ = 1638 (1) Å$^3$, $Z$ = 2, $D_{calc}$ = 1.201 g/cm$^3$. A total of 1785 unique reflections ($2\theta_{max}$ =140.3°) was collected using Cu K$\alpha$ radiation ($\lambda$ = 1.54178 Å). 1730 reflections above 3$\sigma$(I) level were used in the refinement. The structure was solved by the direct method (SHELXS 86). The methine hydrogen of (*S,S*)-**1** and hydroxyl hydrogen of (*S*)-**2** were located by difference-Fourier map, while the others were included at calculated positions. All hydrogen atoms were refined isotropically in the riding mode. Full matrix least squares refinement with 220 variable parameters led to $R$ = 0.043, $Rw$ = 0.058, and GOF = 0.96.

5. 500 ps of molecular dynamics at 300 K using AMBER* force field (MacroModel V4.5, Department of Chemistry, Columbia University, New York) was carried out. During the dynamics run, intermolecular distance constraint between the hydroxyl protons and imino nitrogens and intramolecular torsion constraint involving the OH bond were applied. 500 conformers obtained by 1 ps of sampling interval were subjected to energy minimization, affording a single conformer of the complex.

6. A conformer of the complex was subjected to the preoptimization by semiempirical PM3 calculation. All geometrical parameters were then optimized at the HF/3-21G(*) level. These calculations were conducted by using a program package SPARTAN 4.0 (Wavefunction Inc. California).

7. The synthetic protocol for (*S,S*)-**1** was applied to the preparation of (*S,S*)-**3** from (*R,R*)-*N,N'*-bis(2-nitrobenzyl)tartramide.[2]

8. Crystal data for (*S,S*)-**3**:(*S*)-**2** complex ($C_{20}H_{18}O_2N_4 \cdot C_{20}H_{14}O_2$, *Mr* 632.7): crystal system monoclinic; space group $P2_1$; lattice constants, $a$ = 11.755 (7), $b$ = 12.222 (6), $c$ = 11.673 (5) Å, $\beta$ = 105.26 (4)°, $V$ = 1618 (1) Å$^3$, $Z$ = 2, $D_{calc}$ = 1.299 g/cm$^3$. A total of 3186 unique reflections ($2\theta_{max}$ =140.3°) was collected using Cu K$\alpha$ radiation ($\lambda$ = 1.54178 Å). 2985 reflections above 3$\sigma$(I) level were used in the refinement. The structure was solved by the direct method (SIR 92). The hydroxyl hydrogens of (*S*)-**2** were located by difference-Fourier map, while the others were included at calculated positions. All hydrogen atoms were refined isotropically in the riding mode. Full matrix least squares refinement with 465 variable parameters led to $R$ = 0.042, $Rw$ = 0.054, and GOF = 1.13.

9. X-ray crystal structure of the hydrogen-bonded complex similar to those in the present study was observed in the system consisting of (*S*)-**2** and iminodioxolane-derived chiral receptor.[1d] The fact that three structurally related but different systems provided the same binding motif of the complex supports the conformational preference of the hydrogen-bonded complex discussed here. In addition, geometry optimization (HF/3-21G(*)[6]) of the X-ray crystal structures converged with preserving the hydrogen bonds and proximity between substituents, indicating that the hydrogen-bonded structures were reproducible without the packing effect in the crystalline state.